Short Papers

Accurate Sliding-Mode Control of Pneumatic Systems Using Low-Cost Solenoid Valves

T. Nguyen, J. Leavitt, F. Jabbari, and J. E. Bobrow

***Abstract*—A control law is developed for an inexpensive pneumatic motion control system using four solenoid on/off valves and a position feedback sensor. A sliding-mode approach is used, which is well known for its tolerance for system uncertainties. In contrast to previous control laws, our approach does not use pulsewidth modulation. The control law has an energy-saving mode that saves electrical power, reduces chattering, and prolongs the valve's life. Our simulation and experimental results show that the proposed tracking control law performs very well with good tracking and relatively low steady-state position errors.**

***Index Terms*—Fluid power, pneumatic actuators, pneumatic control, pulsewidth modulation, sliding-mode control.**

I. Introduction

Pneumatic actuation is becoming more popular recently due to decreasing component costs and recent improvements in valve technology. Today's valves are faster, less expensive, and more accurate than valves made previously. Pneumatic actuators are known for their clean operation, high force-to-mass ratio, and easy serviceability. In most previous work, servovalves, rather than solenoid valves, have been used for pneumatic actuation applications. For example, McDonell and Bobrow [1], developed a hierarchical feedback linearized controller for force and position tracking of a pneumatically actuated robot. Surgenor and Vaughan [2] used a servovalve in conjunction with a sliding mode control approach to achieve excellent performance. Other researchers have included the dynamics of the servovalve as part of the control design to achieve higher performance (see, for instance, Richer and Hurmuzlu [3] or Richard and Scavarda [4]).

Unfortunately, servovalves like the ones used in the above-mentioned research are usually expensive because of the high-precision manufacturing needed to produce them and because of the need for a built-in orifice area control circuit. With faster and more accurate valves now available, solenoid on/off valves can potentially be used to replace servovalves. One method for controlling systems with solenoid valves is to use pulsewidth modulation (PWM) to effectively approximate the flow properties of a servovalve with solenoid valves. As a result, it allows control laws derived for servovalves to be used with on/off valves. For example, Shen *et al*. [5] used PWM to create a sliding mode control signal in conjunction with the so-called "equivalent control" signal [6], [7] necessary to keep the system dynamics on the sliding surface. Varseveld and Bone [8] developed several PWM schemes to effectively linearize the relationship between the modulator driving voltage and the load velocity. It was demonstrated in Noritsugu [9] that if this linear relationship is established, the highly nonlinear pneumatic system will be easier to control with a higher level of accuracy.

Our approach implements a sliding-mode control law directly without using PWM. Because we do not have PWM, we can not compute and implement the equivalent control signal mentioned above. Our results demonstrate that the errors caused by this limitation are not large. In order to develop the controller, we used a sliding surface similar to that developed by Surgenor and Vaughan [2], along with an analysis similar to that used by Shen, *et al*. in [5]. Because we do not rely on the equivalent control signal, we are able to significantly reduce valve switching as compared to previous methods. In addition, our approach conserves both air and electrical power, which is important for untethered systems [11]. This is also a primary concern for mobile applications such as the robot of Granosik and Borenstein [10], or in the monopropellant systems such as that developed by Barth *et al*. [12].

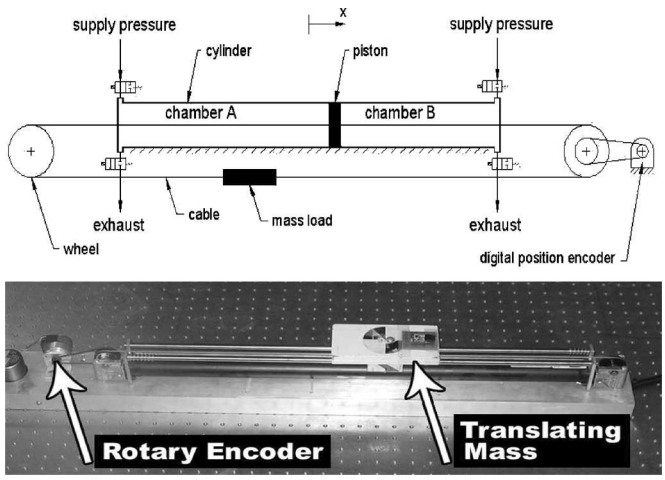

Fig. 1. Diagram and photograph of cable-actuated cylinder and mass with position encoder.

II. Basic Equations of the Actuation System

The pneumatic actuation system used for this research is comprised of a Tolomatic[1] cylinder and four Matrix[2] pneumatic solenoid valves as shown in Fig. 1. The piston is connected to a cable, which drives a translating mass. The double-acting cylinder has equal areas on either side of the piston. In order to describe cylinder air flow dynamics, we assume that we have an adiabatic process, i.e., heat transfer across the control volume boundary is negligible, and that air is an ideal gas. The cylinder flow dynamics in chamber A and chamber B of the cylinder can be approximated by [13] as

$$\dot{P}_A = \frac{r}{V_A}(RT\dot{m}_A - P_A\dot{V}_A) \tag{1}$$

$$\dot{P}_B = \frac{r}{V_B}(RT\dot{m}_B + P_B\dot{V}_B) \tag{2}$$

where P_A, P_B are the pressures inside chambers A, B (Pascal), V_A, V_B are the volumes of chambers A, B (m^3), $\dot{m}_A, \dot{m}_B$ are the mass flow rates in chambers A, B (Kg/s), T_s is the temperature of the supply air (°K), r is the ratio of specific heats for air $(r = \frac{c_p}{c_v} = 1.4)$, and R is the universal gas constant $(R = c_p - c_v = 0.287$ KJ/Kg/°K).

If we let L be the length of the cylinder and A be its cross-sectional area, then the volume V_A becomes $A(\frac{L}{2} + x)$ and the volume of

Manuscript received July 18, 2005; revised November 15, 2005. Recommended by Technical Editor J. R. Wagner.

The authors are with the Department of Mechanical and Aerospace Engineering, University of California, Irvine, CA 92697 USA (e-mail: leavittj@uci.edu; fjabbari@uci.edu; jebobrow@uci.edu).

Digital Object Identifier 10.1109/TMECH.2006.892821

[1][Online]. Available: http/www.tolomatic.com

[2][Online]. Available: http//www.matrix.to.it.default.htm

chamber B, $V_B = A(\frac{L}{2} - x)$. With these volumes, (1) and (2) become

$$\dot{P}_A = \frac{r}{A\left(\frac{L}{2}+x\right)}(RT\dot{m}_A - AP_A\dot{x}) \tag{3}$$

$$\dot{P}_B = \frac{r}{A\left(\frac{L}{2}-x\right)}(RT\dot{m}_B + AP_B\dot{x}). \tag{4}$$

The net mass flow rates into chambers A and B are

$$\dot{m}_A = \dot{m}_{A\_\text{in}} - \dot{m}_{A\_\text{out}} \tag{5}$$

$$\dot{m}_B = \dot{m}_{B\_\text{in}} - \dot{m}_{B\_\text{out}}. \tag{6}$$

The mass flow rate of air through the valve is regulated by the air passage area as the flow through an orifice [14], which is expressed as

$$\dot{m} = \dot{m}(P_{\text{up}}, P_{\text{down}}) = \times \begin{cases} \sqrt{\frac{2r}{r-1}}\sqrt{\left(\frac{P_{\text{down}}}{P_{\text{up}}}\right)^{\frac{2}{r}} - \left(\frac{P_{\text{down}}}{P_{\text{up}}}\right)^{\frac{r+1}{r}}}\frac{C_{\text{val}}\cdot S}{\sqrt{T}}P_{\text{up}}, & \frac{P_{\text{down}}}{P_{\text{up}}} > 0.528 \\ \left(\frac{2}{r+1}\right)^{\frac{1}{r-1}}\sqrt{\frac{2r}{r+1}}\frac{C_{\text{val}}\cdot S}{\sqrt{T}}P_{\text{up}}, & \frac{P_{\text{down}}}{P_{\text{up}}} \le 0.528 \end{cases} \tag{7}$$

where C_{val} is the valve flow rate coefficient, S is the orifice passage area (m^2), P_{up} and P_{down} are the up and down stream pressures, respectively, and T is the gas temperature (°K).

Finally, the dynamics of the piston and the load is simply

$$M\ddot{x} = A\left(P_A - P_B\right) - C_{\text{vis}}\dot{x} - C_{\text{coulomb}}(\text{sign}(\dot{x})) \tag{8}$$

where M is the total mass of the load and piston, A is the cylinder area, C_{vis} is the viscous friction coefficient, and C_{coulomb} is Coulomb friction.

III. Control Design

In order to facilitate the control law design, a switching scheme for the four two-way on/off valves shown in Fig. 1 is defined so that the system will have three modes of operation as follows:

$$\begin{aligned} &\text{mode 1:} \quad \text{chamber } A \text{ fills, chamber } B \text{ exhausts, denoted } u = 1 \\ &\text{mode 2:} \quad \text{chamber } A \text{ exhausts, chamber } B \text{ fills, denoted } u = -1 \\ &\text{mode 3:} \quad \text{air flow into both chambers is blocked, denoted } u = 0. \end{aligned} \tag{9}$$

Mode 1 and 2 are used for changing the direction of the force on the piston, and mode 3 is used to save energy and to avoid chattering when the tracking error is deemed small enough.

Differentiating (8) and using (3)–(7), the system dynamics can be written as:

$$\dddot{x} = \begin{cases} f(z) + b^+(z), & u = 1 \\ f(z) - b^-(z), & u = -1 \\ f(z), & u = 0 \end{cases} \tag{10}$$

where $z \equiv (x, \dot{x}, \ddot{x}, P_A, P_B)$, and

$$f(z) = -\frac{C_{\text{vis}}}{M}\ddot{x} - \frac{Ar}{M}\left[\frac{P_A}{\left(\frac{L}{2}+x\right)} + \frac{P_B}{\left(\frac{L}{2}-x\right)}\right]\dot{x} \tag{11}$$

$$b^+(z) = \frac{rRT}{M}\left[\frac{1}{\left(\frac{L}{2}+x\right)}\dot{m}_{A\_\text{in}} + \frac{1}{\left(\frac{L}{2}-x\right)}\dot{m}_{B\_\text{out}}\right] \tag{12}$$

$$b^-(z) = \frac{rRT}{M}\left[\frac{1}{\left(\frac{L}{2}+x\right)}\dot{m}_{A\_\text{out}} + \frac{1}{\left(\frac{L}{2}-x\right)}\dot{m}_{B\_\text{in}}\right] \tag{13}$$

with $\dot{m}_{A\_\text{in}}, \dot{m}_{A\_\text{out}}, \dot{m}_{B\_\text{in}}$, and $\dot{m}_{B\_\text{out}}$ defined using the notation in (7) with the supply pressure P_S and the atmospheric pressure P_{atm} creating the flow as $\dot{m}_{A\_\text{in}} = \dot{m}(P_S, P_A)$, $\dot{m}_{A\_\text{out}} = \dot{m}(P_A, P_{\text{atm}})$, $\dot{m}_{B\_\text{in}} = \dot{m}(P_s, P_B)$, and $\dot{m}_{B\_\text{out}} = \dot{m}(P_B, P_{\text{atm}})$. Now, define the second-order sliding surface as

$$s = \ddot{e} + 2\zeta\omega\dot{e} + \omega^2 e \tag{14}$$

where $e = x - x_d$ is the tracking error. We selected a second-order surface because (10) is third order, and one derivative of (14) brings the effect of the control on the dynamics s through $\dddot{e}$ and $\dddot{x}$. We will now show that if a valve is used that has a high-enough flow rate, and the control u is selected so that $u = -sign(s)$, the tracking error diminishes according to the second-order dynamics as

$$\ddot{e} + 2\zeta\omega\dot{e} + \omega^2 e = 0. \tag{15}$$

Define the Lyapunov-like function

$$V = \frac{1}{2}s^2. \tag{16}$$

The sliding surface $s \equiv 0$ is reached within a finite time, when the following condition is enforced [6], [7]

$$\dot{V} = s\dot{s} < -\eta|s| \tag{17}$$

for some constant $\eta > 0$. From (14),

$$\dot{s} = \dddot{e} + \ddot{e}2\zeta\omega + \omega^2\dot{e}. \tag{18}$$

For our system (10), (17), and (18) give

$$\dot{V} = \begin{cases} s(b^+ + \gamma), & u = 1 \\ s(-b^- + \gamma), & u = -1 \end{cases} \tag{19}$$

where $\gamma = f - \dddot{x}_d + \ddot{e}2\zeta\omega + \omega^2\dot{e}$. Note from (12) and (13) that b^+ and b^- are positive for all $z(t)$, and that their magnitude can be made as large as desired by choosing a large valve orifice C_{val} in (7). We first assume (we prove this assertion below) that given an $\eta > 0$, we can choose b^+ and b^- such that

$$b^+ + \gamma > \eta \tag{20}$$

$$-b^- + \gamma < -\eta. \tag{21}$$

Now, if $s < 0$, with $u = -sign(s) = +1$, (19) and (20) show that $\dot{V} = s(b^+ + \gamma) < \eta s < 0$. If $s > 0$, (19) and (20) show that $\dot{V} = s(-b^- + \gamma) < -\eta s < 0$. In other words, the sliding condition $\dot{V} < -\eta|s|$ is always satisfied.

In order to show that b^+ and b^- can be selected to satisfy (20) and (21), we need to show that γ is bounded. We start by noting that $s(0)$ is bounded, since x_d and it derivatives and the initial value for x and its derivatives are bounded. Then, using the sliding control law, (17) shows that $\dot{V}(t) < 0$, which ensures that $V(t)$ is not increasing and that s is bounded due to (16). Next, note that (14) establishes a stable input/output transfer function from s to e. Since for linear, time-invariant (LTI) systems this implies bounded input/bounded output (BIBO) stability, $e(t)$ is bounded, so x will remain bounded. Given bounded $P_A - P_B$ and friction, (8) is a first-order ordinary differential equation in $\dot{x}$, which due to damping, results in a decaying (and thus bounded) $\dot{x}$ and, thus, bounded $\ddot{x}$. Since we assume that the reference signal x_d and its derivative are bounded, e and its two derivatives are bounded as well. The only term left in γ to remain bounded is f [defined in (11)], which only requires that $|x|$ remains smaller than $L/2$, which is a physical limitation of the piston's motion inside the cylinder.

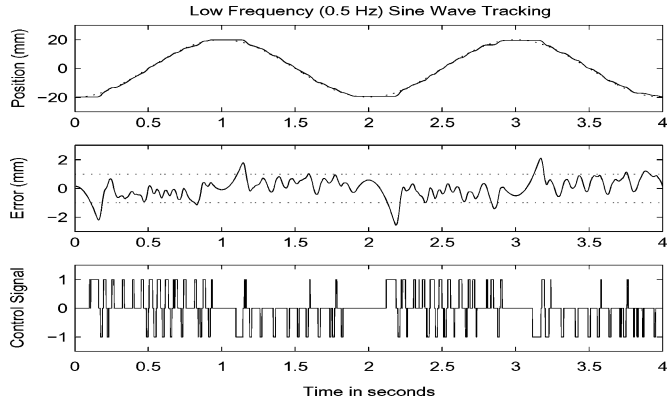

Fig. 2. Top: tracking a 0.5-Hz sine wave. Middle: error signal with dead band. Bottom: control pulses.

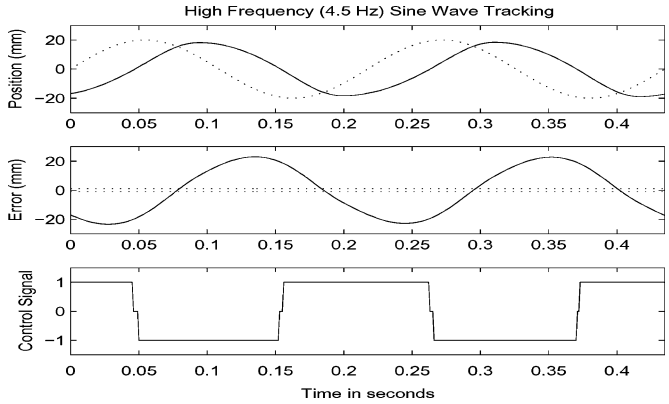

Fig. 3. Top: attempt at tracking a 4.5-Hz sine wave. Middle: error signal. Bottom: control signal is saturated throughout the motion.

In order to reduce control chatter to improve the control law, we define a "dead band" ϵ around zero, and if $|s|$ is within this region, the third mode $u = 0$ is used to save energy. All the flows are stopped by closing all the valves in this mode. Because the sign of $\dot{V}$ is indefinite in this region, some steady-state error exists. The experimental results in the next section demonstrate that ϵ can be selected small enough to achieve an acceptable level of error without causing unnecessary valve chatter. In summary, the control law is

$$\begin{cases} |s| > \epsilon: & u = -\text{sign}(s) \\ |s| \leq \epsilon: & u = 0. \end{cases} \tag{22}$$

This control law will bring the system to the sliding surface $s \equiv 0$ in a finite amount of time, which is determined by the magnitude of η. Once on this surface, the tracking error will decay according to a second-order dynamic system defined by the constants ζ and ω.

IV. Experimental Results

We tested the control law on the hardware shown in Fig. 1. The Tolomatic[1] cylinder model TC10 SK24 has a 25.4-mm bore and a 610.0-mm stroke. The piston is connected to a cable, which drives a translating mass of approximately $M = 2.0$ kg. The four Matrix[2] pneumatic solenoid valves, model BX721108C3JJ, which was used to control the air flow had a response time of approximately 0.007 s, and a flow rate specification of 80 L/min at a pressure drop of 6 bar. The flow rate specification was used to determine C_{val} in (7) with the appropriate operating pressures specified in that formula. We attached a belt-driven rotary encoder to one of the rotating cable pulleys at the end of the cylinder to measure the load position. The resolution was 100.1 counts per millimeter, which is relatively high for the large piston stroke used. The control law was implemented in Matlab's real-time workshop on a P4 PC running at a sampling rate of 500 Hz. The velocity was computed using a backward finite difference of the position signal followed by a second-order 40-Hz Butterworth filter. The acceleration (also needed to compute s) was computed in the same way from the filtered velocity.

After some experimental tuning of the sliding surface parameters, we obtained some excellent results shown in Fig. 2–5. The sliding surface used for this was defined by $\hat{s} = \ddot{e}/\omega^2 + \dot{e}2\zeta/\omega + e$, where $\zeta = 0.15$, and $\omega = 40$ rad/s. For these results, the dead band $\epsilon = 1.0$ was used with the scaled surface $\hat{s}$ rather than s. We found that this scaling made it easier to choose ω, ζ, and ϵ, from the experimental response as follows. When we increased ζ above the stated value of $\zeta = 0.15$, the control seemed to work fine in terms of tracking error,

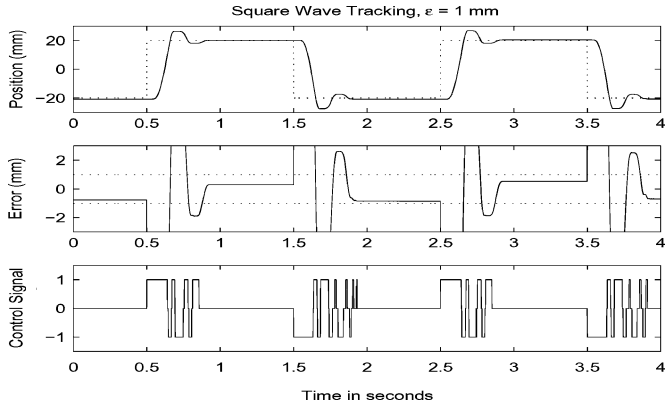

Fig. 4. Top: step response. Middle: error signal with dead band. Bottom: valves do not pulse significantly.

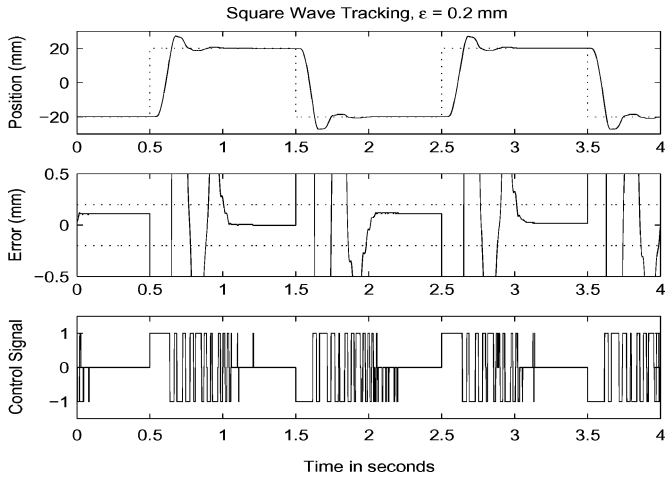

Fig. 5. Top: step response. Middle: small error signal. Bottom: valves pulse more frequently to stabilize with small dead band.

but it chattered more. The problem was that ζ is a coefficient of $\dot{e}$ on the sliding surface, so that noise in $\dot{x}$ is amplified with a large ζ. Similarly, we used a relatively high value for $\omega = 40$ rad/s, because this means that $1/\omega^2$ is small and so, the errors in $\ddot{e}$ of $\hat{s}$ are not amplified as much as would be with a lower ω. Also, since the position-error term in $\hat{s}$ has a coefficient of 1, for a constant input at steady-state, $\hat{s} = e$. This

means that the steady-state error is then directly defined by the value of ϵ in whatever units are used to measure the system position.

Fig. 2 shows the tracking performance of a low-amplitude ± 20-mm sine wave at 0.5 Hz. The dead-band chosen seemed to give a nice trade-off between excessive control action and position error. Remarkably, even though the motion is continuously changing, the valves do not seem to pulse excessively. We also varied the mass M for this experiment from 50% to 400% of its nominal value, and found the resulting motion to be nearly identical to this plot.

The limitation in bandwidth is demonstrated in Fig. 3, where we see that for a 4.5-Hz sine wave reference trajectory, the valves are continuously on in either direction and are unable to produce the flow needed to satisfy the sliding condition. That is, our assumptions in (20) and (21) are not satisfied. Another indication of the performance is the step response as shown in Fig. 4, which also has $\epsilon = 1.0$. Note that good results were obtained without requiring too much pulsing from the valves.

Finally, Fig. 5 demonstrates that very tight position accuracy of about ± 0.1 mm can be achieved at the expense of considerable control action. In this case, the dead band was reduced to $\epsilon = 0.2$. Although this high position accuracy is often desirable, it comes at the expense of extra electrical power consumption in the valves and extra flow from the air supply. This is because each time a solenoid valve opens, electrical energy is used in the solenoid, and extra air flows from the supply to the system.

V. Conclusion

By developing a simple sliding-mode control law, we have used inexpensive components to create a pneumatic actuation system that performs very well. We have demonstrated that the approach only needs simple on/off valves and a position sensor to be implemented. Robustness is achieved with our approach due to its high tolerance for uncertainties in the system dynamics. In addition, the control law only switches the on/off valves when necessary and, therefore, prolongs the valve life and increases the overall reliability of the hardware.

References

[1] B. W. McDonell and J. E. Bobrow, "Modeling, identification, and control of a pneumatically actuated, force controllable robot," *IEEE Trans. Robot. Autom.*, vol. 14, no. 5, pp. 732–742, Oct. 1998.

[2] B. W. Surgenor and N. D. Vaughan, "Continuous sliding mode control of a pneumatic actuator," *Trans. ASME, J. Dyn. Syst., Meas. Control*, vol. 119, pp. 578–581, Sep. 1997.

[3] E. Richer and Y. Hurmuzlu, "A high performance pneumatic force actuator system: Part I and II," *Trans. ASME, J. Dyn. Syst., Meas. Control*, vol. 122, pp. 416–434, 2000.

[4] E. Richard and S. Scavarda, "Comparison between linear and nonlinear control of a electropneumatic servordrive," *Trans. ASME, J. Dyn. Syst., Meas. Control*, vol. 118, pp. 245–252, 1996.

[5] X. Shen, J. Zhang, E. J. Barth, and M. Goldfarb, "Nonlinear averaging applied to the control of pulse width modulated (PWM) pneumatic systems," in *Proc. Amer. Control Conf.*, Jun.–Jul. 2004, vol. 5, pp. 4444–4448.

[6] V. I. Utkin, J. Shi, and J. Gulder, *Sliding Mode Control in Electromechanical Systems*. New York: Taylor & Francis, 1999.

[7] J. J. E. Slotine and W. Li, *Applied Nonlinear Control*. Englewood Cliffs, NJ: Prentice-Hall, 1991.

[8] R. B. van Varseveld and G. M. Bone, "Accurate position control of a pneumatic actuator using on/off solenoid valves," *IEEE/ASME Trans. Mechatronics*, vol. 2, no. 3, pp. 195–204, Jun. 1997.

[9] T. Noritsugu, "Development of PWM mode electro-pneumatic servomechanism, part II: Position control of a pneumatic cylinder," *J. Fluid Control*, vol. 67, pp. 7–28, 1987.

[10] G. Granosik and J. Borenstein, "Minimizing air consumption of pneumatic actuators in mobile robots," in *Proc. IEEE Int. Conf. Robot. Autom.*, New Orleans, LA, Apr. 26–May 1, 2004, pp. 3634–3639.

[11] K. A. Al-Dakkan, M. Goldfarb, and E. J. Barth, "Energy saving control for pneumatic servo systems," in *Proc. IEEE/ASME Int. Conf. Adv. Intell. Mechatron.*, Baltimore, MD, vol. 1, Jul. 20–24, 2003, pp. 284–289.

[12] E. J. Barth, M. A. Gogola, and M. Goldfarb, "Modeling and control of a monopropellant-based pneumatic actuation system," in *Proc. IEEE Int. Conf. Robot. Autom.*, Taipei, Taiwan, vol. 1, Sep. 14–19, 2003, pp. 628–633.

[13] S. Liu and J. E. Bobrow, "An analysis of a pneumatic servo system and its application to a computercontrolled robot," *Trans. ASME, J. Dyn. Syst., Meas. Control*, vol. 110, pp. 228–235, 1988.

[14] J. A. Roberson and C. T. Crowe, *Engineering Fluid Mechanics*. Boston, MA: Houghton Mifflin, 1990.

Systematic Modeling for Free Stators of Rotary Piezoelectric Ultrasonic Motors

Hamed Mojallali, Rouzbeh Amini, Roozbeh Izadi Zamanabadi, and Ali A. Jalali

***Abstract*—This paper presents an equivalent circuit model with complex numbers that describes the free stator model of traveling-wave ultrasonic motors. The mechanical, dielectric, and piezoelectric losses associated with the vibrator are considered by introducing the imaginary part to the equivalent circuit elements. The determination of the complex circuit elements is performed by using a new, simple iterative method. The presented method uses information about five points of the stator admittance measurements. The accuracy of the model in fitting to the experimental data is verified by using the measurements of a recently developed piezoelectric motor and a well-known USR60.**

***Index Terms*—Equivalent circuit, modeling, ultrasonic motor.**

I. Introduction

The advantages and various applications of traveling-wave ultrasonic motors (USMs) have attracted more research attention, compared to the other types of USMs [1]. The driving principle of the traveling-wave USM is based on generating acoustic traveling waves in the stator and producing an elliptic motion of the particles at the surface of the stator and, hereby, driving the rotor by means of friction. Thus, deriving the model of the stator is the first step of the modeling process, which is helpful in order to estimate the electromechanical characteristic of the whole motor and the power supply design for USM. Existing approaches for modeling of USMs are mainly based on equivalent circuit method [1]–[4], analytical approaches [5], or finite-element method (FEM) [6]. Although FEM provides the possibility of a precise study on different mechanical parts of the motor, it is inconvenient due to computational cost. Likewise, electrical parameters

Manuscript received March 21, 2006; revised May 20, 2006. Recommended by Technical Editor M.-C. Tsai.

H. Mojallali and A. A. Jalali are with the Electrical Engineering Department, Iran University of Science and Technology, 16846 Tehran, Iran (e-mail: mojallali@iust.ac.ir; ajalali@iust.ac.ir).

R. Amini is with the Department of Aerospace Engineering, Technical University of Delft, 2600 Delft, The Netherlands (e-mail: R.Amini@tudelft.nl).

R. Izadi-Zamanabadi is with the Control Engineering Department, Aalborg University, 9220 Aalborg, Denmark (e-mail: riz@control.aau.dk).

Digital Object Identifier 10.1109/TMECH.2006.892829